ISSN 0915-633X

NATIONAL INSTITUTE FOR FUSION SCIENCE

Virtual Cathode in a Spherical Inertial Electrostatic Confinement Device

H. Momota and G.H. Miley

(Received - Jan. 29, 2001)

NIFS-682 Feb. 2001

RESEARCH REPORT
NIFS Series

TOKI, JAPAN

Virtual Cathode in a Spherical Inertial Electrostatic Confinement Device

Hiromu Momota* and George H. Miley

Dept. Nuclear, Plasma, and Radiological Engineering, University of Illinois at Urbana-Champaign,
214 Nuclear Engineering Lab. 103 S. Goodwin Avenue, Urbana, IL 61801, USA
*: Professor Emeritus, National Institute for Fusion Science,
322-6 Oroshi, Toki, Gifu 5095292, Japan

ABSTRACT

"Double-well" potential structure (virtual cathode formation) is studied in a spherical inertial electrostatic confinement (SIEC) device using non-linear Poisson's equation. Particle densities are derived from a kinetic equation equivalent to Vlasov's equation. Velocities of collision-free electrons and ions at the edge of the configuration will be almost aligned towards the center; however, they have small divergences. Analyses show appearance of a virtual cathode potential well relevant to burn fusion fuels near the center of SIEC.

KEYWORDS: non-neutral equilibrium, spherical inertial electrostatic confinement, Vlasov equilibrium, non-linear Poisson's equation,

1. INTRODUCTION

Spherical Inertial Electrostatic Confinement (SIEC) provides one of the simplest candidates among various fusion approaches for controlled fusion [1]. Fig.1 shows a cross section of a single-grid spherical IEC. It has no externally applied magnetic field and ions are focused using an electrostatic field to accelerate ions towards the spherical center of the unit. Consequently a very high-density core of fuel ions is produced in the center region, significantly enhancing fusion reactions. The resulting high density of ions produces a high potential hill, which could decrease the kinetic energy of incoming ions. However, electron effects will theoretically change the potential shape in such a way as to reduce or avoid this problem [2]. For a fusion device, the predicted appearance of a deep potential well inside the potential hill is beneficial in the sense of creating a "trap" for ions where a high fusion rate would occur. Discussions on this virtual cathode, however, are continuing since Hirsch only considered a simple case where the charged particles are monoenergetic and have no angular momentum. Analyses including angular momentum have been reported [3-7], but these studies introduced various limiting assumptions or have been completely numerical such that the underlying phenomena were obscured.

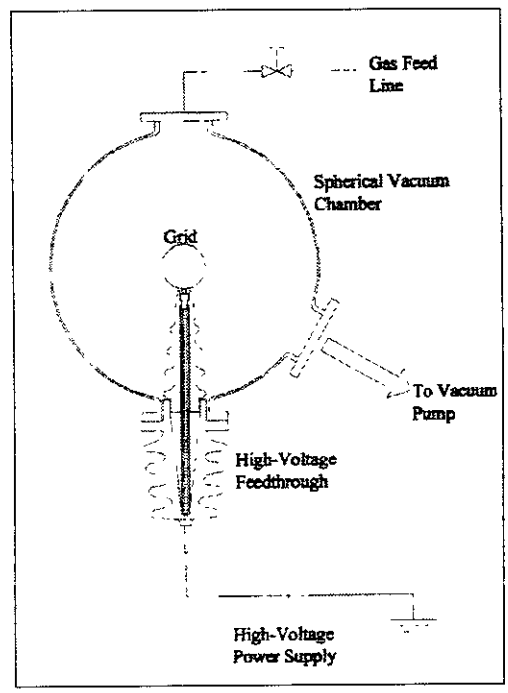

Fig.1: Cross sectional view of a spherical IEC

In several recent experiments, a virtual cathode structure inside of the potential hill has been observed

adding confidence in the existence of these important phenomena [8,9]. (see Fig.2). It is the purpose of this paper to further clarify the mechanism of the virtual cathode and to find out the conditions for its formation.

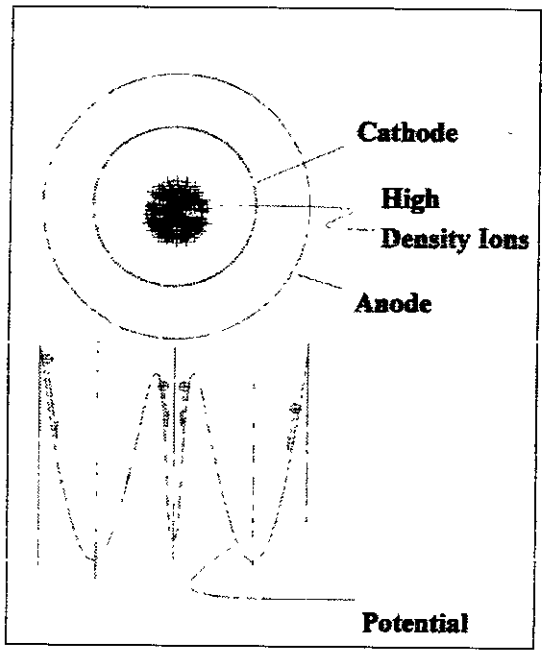

Fig.2: Potential structure develops in the non-neutral plasma, creating virtual cathode

We will discuss the steady state where electron collisions are so rare that a collision-free kinetic equation can be used. Ions are collision-free too and their velocity vector is allowed to diverge away from the center by a small angle (i.e. we have "angular momentum").

2. DISTRIBUTION FUNCTION

Consider a charged particle located at $(\vec{r}_0, \vec{v}_0)$ on the 6-dimensional phase space at the time t_0 and $(\vec{r}, \vec{v})$ at the time t. Since we are prospecting for nuclear fusion, the mean kinetic energy of particles is assumed so high that collisions between particles can be ignored in determining their motion. Then, collision-free Vlasov's equation for the distribution function is relevant to describe the spherically symmetric plasma in a steady state:

$$\left(v_r \frac{\partial}{\partial r} + \left.\frac{d\vec{v}}{dt}\right|_r \frac{\partial}{\partial v_r} + \left.\frac{d\vec{v}}{dt}\right|_\perp \frac{\partial}{\partial v_\perp} \right) f_s(r, v_r, v_\perp) = 0 . \qquad (1)$$

The subscript s and $\perp$ denote species of particles and the components perpendicular to the radial direction. In our stationary state, the total energy and the canonical angular momentum conserve. The velocity is expressed in terms of the radius r. The left hand side on the Eq. (1) takes, accordingly, a form of a total deferential with respect to the radius r:

$$\frac{d}{dr} f_s(r, v_r, v_\perp) = 0 . \qquad (2)$$

The subscript s represents the species of particles.

With these constants of motion, the particle motion connects the two particle distribution functions at the different radius. Consider a charged particle located at $r = r_0$ and $r = r$. By use of the constants of motions, the total energy H_s and the angular momentum $P_{s\perp}$, a particle's radial velocity v_r and perpendicular velocity $v_\perp$ at the radius r can be denoted by corresponding velocities v_{r0} and $v_{\perp 0}$ at r_0:

$$\begin{aligned} v_{\perp 0} &= \frac{P_{s\perp}}{M_s r_0} \equiv \frac{r}{r_0} v_\perp \\ v_{r0} &= \sqrt{\frac{2}{M_s}} \sqrt{H_s - q_s \varphi_0 - M_s v_\perp^2 r^2 / 2 r_0^2} \end{aligned} . \qquad (3)$$

Here $\varphi(r)$ and φ_0 are the electrostatic potentials at positions $r = r$ and $r = r_0$, respectively. The equation states that the particle density keeps its value as constant along the trajectory on the 6-dimensional phase space. Therefore, we have:

$$f_s(r, v_r, v_\perp) = f_s(r_0, v_{r0}, v_{\perp 0}) . \qquad (4)$$

Combining equations (3) and (4), the distribution function at a position r is given in a simple form:

This approach is equivalent to the formula given by Nevins [10], where the distribution function is represented in terms of constants of motion such as the total energy and the angular momentum. Expression (4), however, connects the distribution function rather explicitly to that of grid region.

3. STEADY STATE SOLUTION

In experimental devices, ions are generated by a plasma discharge outside the spherical grid, which is negatively

biased. Thus ions are accelerated by the grid and pass through it going towards the center. Ions arrive at the central region and then turn back to their birth potential, where they stop and are re-accelerated back towards the center. The spherical symmetry of the electrostatic field near the grid region is, however, perturbed due to the discrete structure of the grid. This asymmetric electric field near the grid gives the ion beam a certain divergence. To represent this effect, let the divergence of the ion velocity vector from the radial vector be Δ_s at the grid. The distribution function of ions at $r = a$ will be assumed to be the form:

$$f_s(a, v_r, v_{\perp a}) = \frac{n_{sa}}{2\pi v_a^2}\delta(|v_a| - V_s)\frac{1}{\Delta_s^2}\exp(-\gamma_a^2/\Delta_s^2) \qquad (5)$$

$$\sin\gamma \equiv \frac{v_\perp}{v},$$

where a is the radius of the inner grid. The quantity V_s denotes the particle velocity of s-species at the inner grid. Using characteristics of delta-function, the distribution function at $r = r$ is found as:

$$f_s(r, v_r, v_\perp) = \qquad (6)$$
$$\frac{n_{sa}}{2\pi v_a}\sqrt{\frac{M_s}{2}}\frac{\delta(v_r - \sqrt{2[H_s - q_s\varphi(r)]/M_s - v_\perp^2})}{\sqrt{H_s - q_s\varphi(r) - M_s v_\perp^2/2}}$$
$$\times\frac{1}{\Delta_s^2}\exp\left[-\frac{v_\perp^2}{2(H_s - q_s\varphi_a)\Delta_s^2 a^2/M_s r^2}\right].$$

This result shows that the divergence of the ions is larger near the spherical center than at the grid region, providing that electrostatic potential effects can be ignored.

The ion density profile is obtained by integrating this equation over velocity space, giving:

$$n_s(r) = \sqrt{\frac{H_s - q_s\varphi_a}{H_s - q_s\varphi(r)}}\frac{n_{sa}a^2}{r^2 D_s^2(r)}\int_0^1 \frac{\exp[-\xi/D_s^2(r)]}{\sqrt{1-\xi}}d\xi \qquad (7)$$

where, $D_s^2(r) \equiv \frac{\Delta_s^2 a^2}{r^2}\frac{H_s - q_s\varphi_a}{H_s - q_s\varphi(r)}$

Discussions so far presented are applicable in a limiting case where particles suffer no collisions. The collision frequency between electrons is generally much larger than that of ions. Thus within a SIEC in a present laboratory, the electrons might suffer from a large self-collision. Throughout the present paper, however, we will discuss a case in which particle collision is negligibly small and consequent ion distribution functions are given by Eq. (6).

An electrostatic potential of this steady state is determined by Poisson's equation:

$$-\varepsilon_0\frac{1}{r^2}\frac{d}{dr}\left[r^2\frac{d\varphi}{dr}(r)\right] = Zen_i(r) - en_e(r). \qquad (8)$$

This equation is supplemented by the equations for particle density given in equation (7) as a function of the electrostatic potential. The quantity Z stands for the charge number of the ion and we will henceforth put it equal to unity for the simplicity. Equation (8) and supplemented Eq. (7) for the particle density are a couple of complicated nonlinear differential equations and we are disable to obtain the analytical solution. A certain numerical calculation is, therefore, needed to study the detail of the virtual cathode.

4. NUMERICAL RESULTS

In carrying out numerical calculations, we will employ the following model:

(a) The electrostatic potential φ_a at $r = a$ (a is the radius of spherical grid) is approximately the same as the voltage $-V_g$ applied to the spherical grid. This condition gives us one of the needed boundary conditions for obtaining a solution to Poisson's equation.
(b) Ions are first produced outside the grid region where the electrostatic potential is zero. The total energy of ions is therefore zero.
(c) Concerning electron birth, we are considering two opposite cases. In the first case, electrons are completely collision-free and their births are at $r = a$ with a small radial velocity εeV_g. Then the total energy of electron is $eV_g(\varepsilon + 1)$. The ratio of electron density to the ion density at the grid region is a controllable variable.
(d) The divergenceΔ of ions is 0.2 at the grid region.

The boundary conditions for Poisson's equations are:

$$\varphi(a) = -V_g$$
$$\frac{d\varphi}{dr}(a) = -\frac{e^2}{\varepsilon_0}\int_0^a [n_i(\rho) - n_e(\rho)]\,\rho^2\,d\rho. \qquad (9)$$

We introduced an approximated formula for the integral in Eq. (8):

$$\int_0^1 \frac{\exp(-\eta^2 t)}{\sqrt{1-t}} dt \approx 2\exp\left(-\frac{5}{4}\eta^2\right) + \frac{\eta^2}{1+\eta^4} \qquad (10)$$

which simplifies the calculation significantly. A set of integral-differential equation is reduced to a differential equation.

Results of numerical calculations are exhibited in Fig.3 to Fig.7 for a various densities of ions and electrons at the grid region. The solid lines and broken line denote respectively the number density of ions and electrons. Densities and potential are normalized by quantities $ea^2 n_i(a)/\varepsilon_0 V_g$ and V_g, respectively. The scales of the horizontal axis are multiplied by a factor *1000.*

The potential hill is low in a case of low edge density and ions and electrons form easily a peak at the center. (Fig.3). As the density at the edge increases, the potential hill develops and focusing of ions decreases. (Fig.4). In a case of edge density being nearly $0.8 \times \varepsilon_0 V_g / ea^2$, potential hill near the center is almost V_g and rejected ions form a second bump out of the central area. Throughout calculations under the condition that the electron number density at the edge $n_i(a)$ is equal that of ions $n_e(a)$; well depth of the potential at the center is

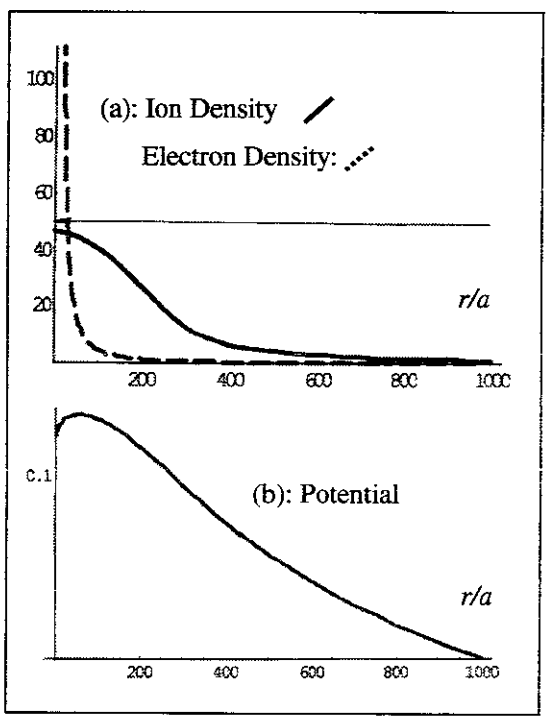

Fig.3: Radial profile of density (a) and potential (b) for low edge density [$n_i(a) = 0.2 \times \varepsilon_0 V_g / ea^2$, $ne(a) = ni(a)$]

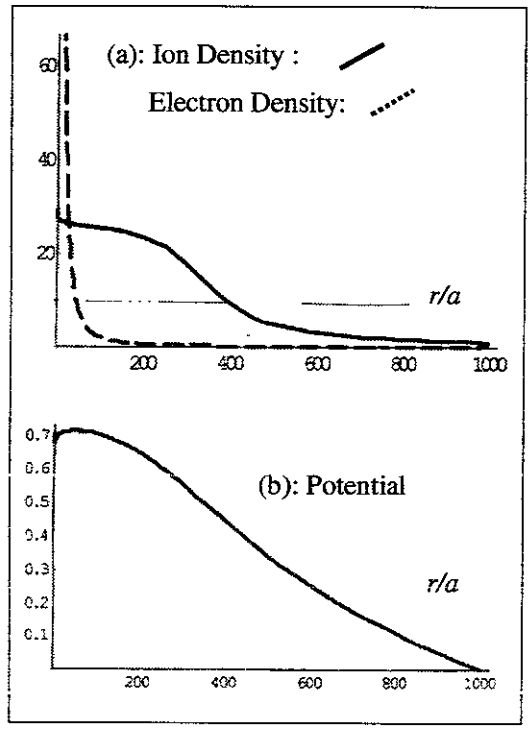

Fig.4: Radial profile of density (a) and potential (b) for intermediate edge density [$n_i(a) = 0.5 \times \varepsilon_0 V_g / ea^2$, $ne(a) = ni(a)$]

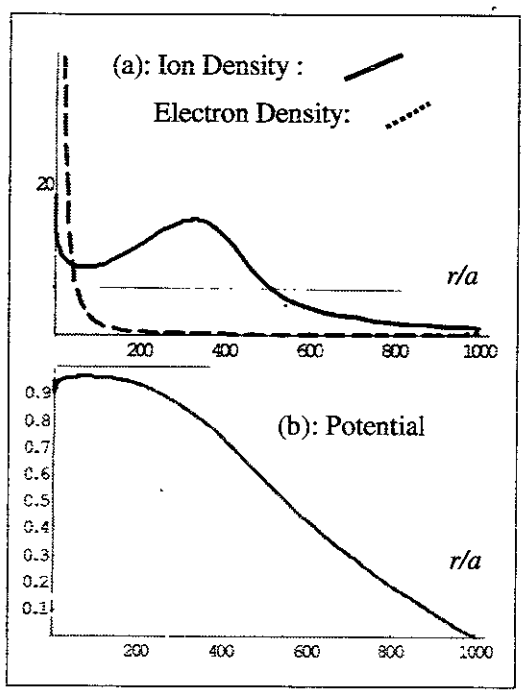

Fig.5: Radial profile of density (a) and potential (b) in a case of high edge density [$n_i(a) = 0.8 \times \varepsilon_0 V_g / ea^2$, $ne(a) = 1.0\, ni(a)$]

inappreciable. In a case of edge number density being

larger than $\varepsilon_0 V_g/ea^2$, we have no real solution, i.e. solutions take complex value and extremely sensitive to the boundary condition.

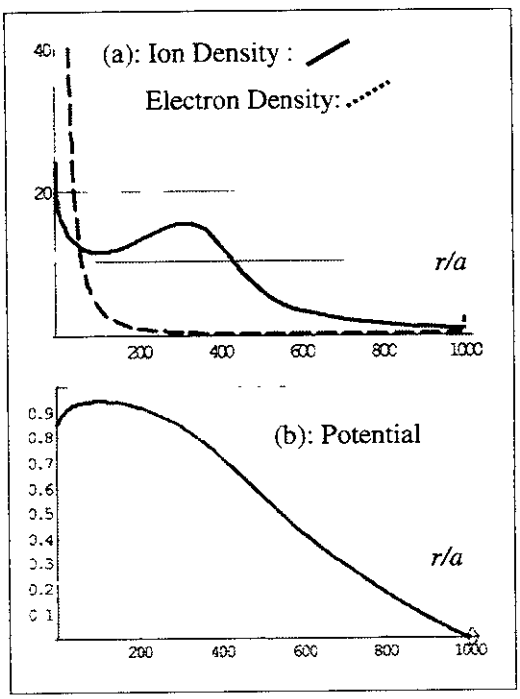

Fig.6: Radial profile of density (a) and potential (b) in a case of high edge density [$n_i(a) = 0.8 \times \varepsilon_0 V_g/ea^2$, $ne(a) = 2.5\ ni(a)$]

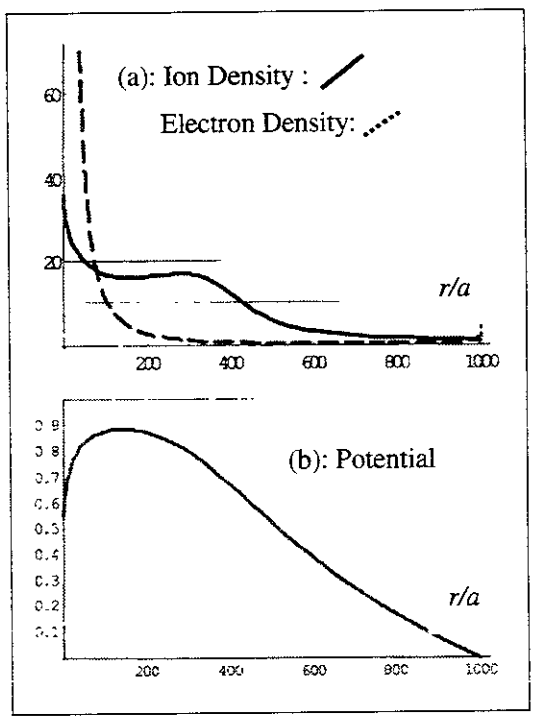

Fig.7: Radial profile of density (a) and potential (b) in a case of high edge density [$n_i(a) = 0.8 \times \varepsilon_0 V_g/ea^2$, $ne(a) = 6.0\ ni(a)$]

In cases of a higher edge density, no potential well appears, and a second hill of the ion density profile appears out of the center. It is shown that the situation changes, however, once one provides a larger edge density of electrons compared with that of ions. In Fig.6 where the electron edge density $n_e(a)$ is 2.5 times the ion edge density $n_i(a)$, one finds the ion density increases near the center and evidence of a potential well at the center. We are able to obtain a real solution for a steady state up to the case of electron edge density to be 6 times of ions. (Fig.7). The second bump of ion density is eliminate and an appreciable potential well appears at the spherical center. We have no real solution also in the case of an ion edge density higher than the value $\varepsilon_0 V_g/ea^2$.

5. CONCLUSIONS AND DISCUSSIONS

We have studied double structure or virtual cathode formation of a spherical inertial electrostatic confinement. The study concerns particle's distribution with divergence Δ of the direction of the velocity around the center and addition of edge electron density.

(a) Small angular momentum of both ions and electrons creates a certain virtual cathode in a potential hill near the spherical center of SIEC.

(b) The potential hill is, however, small if the density parameter $en_{ia}a^2/\varepsilon_0 V_g$ is much smaller than unity.

(c) If the density parameter $en_{ia}a^2/\varepsilon_0 V_g$ approaches to unity, the potential hill becomes appreciable. This causes the large second bump in the density profile. No potential bump or virtual anode, however, appears associated with the ion bump.

(d) Increased electron density at the grid region creates an appreciable potential well (virtual cathode) inside the potential hill.

(e) No ion hole appears in the potential well, but ion density peaks at the potential well.

Conclusions of these studies are applicable only over a restricted parameter region. For cases where the density Parameter $en_{ia}a^2/\varepsilon_0 V_g$ is larger than unity, no real solution to the nonlinear Poisson equation has been

obtained.

It becomes obvious that the electrons play an important role in creating a virtual cathode. Nevertheless, detailed studies on the electron distribution function are needed to estimate precisely the laboratory SIEC. The development of a method that provides enough electron density at the grid is inevitable.

The density limit: $en_{i_2}a^2 / \varepsilon_0 V_g < 1$ for a real steady solution might restrict the power level of the steady SIEC unit to a lower one. In this paper, we ignored all inter-particle collisions. However, further studies on a collisional equilibrium state of related fueling and loss processes are essential to understand and evaluate the complete picture for a SIEC.

ACKNOWLEDGEMENTS

This work was carried out as a collaborating research of the National Institute for Fusion Science.

REFERENCES

[1] HIRSCH, R.L.J. *Appl. Physics* **38**, 4522 (1969).

[2] OHNISHI, M., YAMAMOTO Y., YOSHIKAWA K., and SATO K., "Multi-Potential Well Formation and Neutron Production in Inertial-Electrostatic Confinement Fusion by Numerical Simulations," in *Proceedings of 16th IEEE/NPSS Symposium on Fusion Energy* Vol.2 (1995), 1468-1471.

[3] HU, K. M. and KLEVANS, E. H., *Phys. Fluids* **17** (1974), 227-231

[4] CHERRINGTON B. E. et al., Annals New York Academy of Sciences.

[5] TZONEV, I. V., MILEY, G. H., and NEBEL, R. A., "A Computational Study of the Convergence of Large Angular Momentum, High Current Ion Beams in an Inertial Electrostatic Confinement (IEC) Device," *International Conference on Phenomena in Ionized Gases XXII* **4** (1995), 197-198

[6] SATSANGI, A. J., "Light Intensity Measurements of an Inertial Electrostatic Confinement Fusion Plasma," M.S. thesis, Department of Nuclear Engineering, University of Illinois at Urbana-Champaign, 1996.

[7] NEVINS, W. M. *Phys. Plasma* **2**, 3804 (1995)

Recent Issues of NIFS Series

NIFS-660 I Watari, I Mutoh, R Kumazawa, I Seki, K Saito, Y Torii , Y P Zhao , D Hartmann , H Idei, S Kubo K Ohkubo, M Sato, I Shimozuma Y Yoshimura, K Ikeda, O Kaneko, Y Oka, M Osakabe, Y Takeiri, K Tsumori, N Ashikawa , P C deVries M I moto A Fukuyama , H Funaba, M Goto, K Ida, S Inagaki, N Inoue, M Isobe, K Itoh, S Kado, K Kawahata, T Kobuchi, K Khlopenkov, A Komori, A Krasilnikov , Y Liang,S Masuzaki, K Matsuoka, I Minami, J Miyazawa, T Morisaki, S Morita, S Murakami, S Muto Y Nagayama, Y Nakamura H Nakanishi, K Narihara, K Nishimura, N Noda A TNotake, S Ohdachi, N Ohyabu, H Okada , M Okamoto, T Ozaki, R O Pavlichenko, B J Peterson, A Sagara, S Sakakibara, R Sakamoto, H Sasao, M Sasao, K. Sato S Satoh, T Satow M Shoji, S Sudo, H Suzuki, M Takechi, N Tamura ,S Tanahashi, K Tanaka, K Toi, I Tokuzawa, K Y Watanabe, T Watanabe, H Yamada I Yamada, S Yamaguchi, S Yamamoto, K Yamazaki, M Yokoyama, Y Hamada, O Motojima, M Fujiwara,
The Performance of ICRF Heated Plasmas in LHD Sep 2000
(IAEA-CN-77/EX8/4)

NIFS-661 K Yamazaki, K Y Watanabe, A Sagara, H Yamada, S Sakakibara, K Narihara, K Tanaka, M Osakabe, K Nishimura, O Motojima, M Fujiwara, the LHD Group,
Helical Reactor Design Studies Based on New Confinement Scalings Sep 2000
(IAEA-CN-77/ FTP 2/12)

NIFS-662 T Hayashi, N. Mizuguchi, H Miura and T Sato,
Dynamics of Relaxation Phenomena in Spherical Tokamak Sep 2000
(IAEA-CN-77THP2/13)

NIFS-663 H Nakamura and T. Sato, H. Kambe and K. Sawada and T Saiki,
Design and Optimization of Tapered Structure of Near-field Fiber Probe Based on FDTD Simulation Oct 2000

NIFS-664 N Nakajima,
Three Dimensional Ideal MHD Stability Analysis in L=2 Heliotron Systems Oct 2000

NIFS-665 S Fujiwara and T. Sato,
Structure Formation of a Single Polymer Chain. I Growth of trans Domains. Nov 2000

NIFS-666 S Kida,
Vortical Structure of Turbulence: Nov 2000

NIFS-667 H Nakamura, S Fujiwara and T Sato,
Rigidity of Orientationally Ordered Domains of Short Chain Molecules Nov 2000

NIFS-668 T Mutoh, R Kumazawa, T Seki, K. Saito, Y Torii, F Shimpo, G Nomura, T Watari, D A Hartmann, M. Yokota, K Akaishi, N Ashikawa, P deVries, M Emoto, H Funaba, M Goto, K Ida, H Idei, K Ikeda, S Inagaki, N Inoue, M Isobe, O. Kaneko, K Kawahata, A Komori, T Kobuchi, S Kubo, S. Masuzaki, T Morisaki, S Morita, J Miyazawa, S Murakami, T Minami, S Muto, Y Nagayama, Y Nakamura, H Nakanishi, K. Narihara, N Noda, K Nishimura, K Ohkubo, N Ohyabu, S Ohdachi, Y. Oka, M Osakabe, T Ozaki, B J Peterson, A Sagara, N. Sato, S Sakakibara, R Sakamoto, H Sasao, M Sasao, M Sato, T Shimozuma, M Shoji, S Sudo, H Suzuki, Y Takeiri, K Tanaka, K. Toi, T Tokuzawa, K. Tsumori, K Y Watanabe, T Watanabe, H Yamada, I Yamada, S Yamaguchi, K Yamazaki, M. Yokoyama, Y Yoshimura, Y Hamada, O Motojima, M Fujiwara,
Fast- and Slow-Wave Heating of Ion Cyclotron Range of Frequencies in the Large Helical Device Nov 2000

NIFS-669 K. Mima, M S Jovanovic, Y. Sentoku, Z-M Sheng, M M Skoric and T Sato,
Stimulated Photon Cascade and Condensate in Relativistic Laser-plasma Interaction Nov 2000

NIFS-670 L Hadzievski, M M Skoric and T. Sato,
On Origin and Dynamics of the Discrete NLS Equation Nov 2000

NIFS-671 K Ohkubo, S. Kubo, H Idei, T Shimozuma, Y Yoshimura, F Leuterer, M Sato and Y Takita,
Analysis of Oversized Sliding Waveguide by Mode Matching and Multi-Mode Network Theory Dec 2000

NIFS-672 C Das, S Kida and S Goto,
Overall Self-Similar Decay of Two-Dimensional Turbulence Dec 2000

NIFS-673 L A Bureyeva, T Kato, V.S Lisitsa and C Namba,
Quasiclassical Representation of Autoionization Decay Rates in Parabolic Coordinates Dec 2000

NIFS-674 L A Bureyeva, V.S Lisitsa and C Namba,
Radiative Cascade Due to Dielectronic Recombination Dec 2000

NIFS-675 M F.Heyn, S V Kasilof, W Kernbichler, K Matsuoka, V V Nemov, S Okamura, O S Pavlichenko,
Configurational Effects on Low Collision Plasma Confinement in CHS Heliotron/Torsatron, Jan 2001

NIFS-676 K. Itoh,
A Prospect at 11th International Toki Conference - Plasma physics, quo vadis?; Jan 2001

NIFS-677 S Satake, H. Sugama, M Okamoto and M Wakatani,
Classification of Particle Orbits near the Magnetic Axis in a Tokamak by Using Constants of Motion, Jan 2001

NIFS-678 M Tanaka and A Yu Grosberg,
Giant Charge Inversion of a Macroion Due to Multivalent Counterions and Monovalent Coions Molecular Dynamics Studyn, Jan 2001

NIFS-679 K Akaishi, M Nakasuga, H Suzuki, M Iima, N Suzuki, A Komori, O Motojima and Vacuum Engineering Group,
Simulation by a Diffusion Model for the Variation of Hydrogen Pressure with Time between Hydrogen Discharge Shots in LHD, Feb 2001

NIFS-680 A Yoshizawa, N Yokoi, S Nisizima, S -I. Itoh and K Itoh
Variational Approach to a Turbulent Swirling Pipe Flow with the Aid of Helicity, Feb 2001

NIFS-681 Alexander.A.Shishkin
Estafette of Drift Resonances, Stochasticity and Control of Particle Motion in a Toroidal Magnetic Trap, Feb. 2001

NIFS-682 H Momota and G H Miley,
Virtual Cathode in a Spherical Inertial Electrostatic Confinement Device, Feb 2001